



STATISTICAL ANALYSIS AND CHEMOMETRIC METHODS

# A Histogram-Based Technique for Simultaneous Colorimetric Determination of Malachite Green and Brilliant Green Using Triton X-100 Micelle

Negar Qashqai \* and Tahereh Heidari 

Ferdowsi University of Mashhad, Faculty of Sciences, Department of Chemistry, Mashhad, Iran

\*Corresponding author's e-mail: negar.qashqai@gmail.com

## Abstract

**Background:** Malachite green (MG) and brilliant green (BG) are two synthetic triphenylmethane dyes with applications in the textile and aquaculture industries. They are considered to be environmental contaminants due to their carcinogenic and mutagenic properties. Both dyes have the same bluish-green color in aqueous solutions.

**Objective:** The aim of this study is to develop a colorimetric analysis as a very simple and cost-effective method to determine the residues of MG and BG simultaneously in aqueous industrial samples.

**Method:** This method is based on the alterations in red, blue, green (RGB) color histograms of the dyes in the presence and absence of Triton X-100 micelle. The images of the samples were taken by a digital camera and converted to the RGB color system using MATLAB software. Partial least-squares regression as a powerful chemometrics tool was used for multivariate calibrations and quantitative measurements. The performance of the proposed method was compared with a simple spectrophotometric method as a reference.

**Results:** Relative errors of prediction for colorimetric and spectrophotometric analysis, respectively, in micellar media were 6.56 and 4.61% for MG and 6.38 and 5.24% for BG. The shortest linear ranges for colorimetric and spectrophotometric analysis, respectively, in micellar media were 0.1–10 and 0.5–5 mg/L for MG and 0.1–15 and 0.5–6 mg/L for BG. The recovery percentages obtained from the analysis of the dyes in real samples of fish-pond water and textile wastewater ranged between 91 and 107%.

**Conclusions:** The good correlation between the results of the colorimetric analysis and the spectrophotometric analysis indicates the reliability of the proposed colorimetric method. Also, the results of the relative recovery study showed insignificant matrix effect.

**Highlights:** This study demonstrates the ability of the colorimetric analysis coupled with chemometrics tools for simultaneous determination of the analytes even with nearly identical colors.

Simple methods of chemical analysis that are handled with lower expenses and technical skills are always in demand (1–6). Such methods enable scientists to efficiently study different chemical systems in a very short time. Among these methods, colorimetric methods are considered very simple, rapid, cost-effective, and precise ways of analysis for a large variety of compounds. There are different techniques for qualitative and

quantitative colorimetric analysis, and, recently, they all have received much attention due to the benefits mentioned above. In some cases, the analyte interacts with a chemical reagent, resulting in a change in the color (7, 8). In other cases, the intensity of the analyte's color is directly measured (9). For any type of measurement, digital images taken by a camera, a scanner, or a cell phone are usually the source of the required data, and

Received: 12 September 2022; Revised: 3 December 2022; Accepted: 14 January 2023

© The Author(s) 2023. Published by Oxford University Press on behalf of AOAC INTERNATIONAL. All rights reserved.

For permissions, please email: journals.permissions@oup.com

they later undergo the image processing steps (10–12). The strategies for image-based colorimetric analysis are based on the type of data acquired from the image—for instance, mean pixel values of the red, blue, green (RGB) channel or cyan, magenta, yellow, black (CMYK) channel (13, 14), RGB color histogram (15), hue, saturation, value (HSV) color space (13), or grayscale image data (16). However, in simultaneous measurement of a series of analytes, colorimetric analysis may face some limitations when the colors of the analytes are very similar to one another. MG and BG are two synthetic dyes that can be an example of such, as they are chromatically identical and almost indistinguishable to the naked eye (Figure 1).

MG and BG are two cationic triphenylmethane dyes that are well-known for their usage in textile industries as coloring agents (17, 18). These dyes exhibit some antifungal, antibacterial, and antiparasitic properties and have a broad application in aquaculture industries for disinfection and treatment of certain fish diseases (19, 20). It has been proven that MG and BG are mutagenic and carcinogenic; therefore, releasing them in natural environments can be harmful for human beings and other biological species (21, 22). There are several methods for removal of the above-mentioned dyes from aqueous solutions by using different materials such as coffee beans (18), carbon-based adsorbents (23), bagasse fly ash (24), or rice husk ash (25), and industries are highly encouraged to use a method for treatment of their wastewater. Thus, it is important to determine the residues of these dyes in aquaculture products and industrial effluents. To date, several methods have been carried out for simultaneous determination of MG and BG, such as liquid chromatography-tandem mass spectrometry (LC-MS/MS) in

aquaculture products (26), ultrahigh-performance liquid chromatography-tandem mass spectrometry (UHPLC-QqQ-MS/MS) in seafood (27), and laser wave-mixing detection interfaced to capillary electrophoresis in aquatic environments (28).

As discussed above, applying colorimetric analysis for simultaneous determination of MG and BG is problematic due to the high similarity between the colors of these dyes. Herein, we offer a novel approach to resolve this problem using the RGB color histogram of the dyes combined with partial least-squares (PLS) regression. PLS is a powerful regression model that is commonly used to calibrate different types of chemical data. The basis of the PLS regression can be found in the literature (29). The analysis of the dyes was simply performed in a light box with a digital camera as a detector. The dyes were also analyzed using an ultraviolet-visible (UV-Vis) spectrophotometer as a reference method to compare with the proposed colorimetric method. In the final step, we examined our proposed method on some real industrial samples.

## Experimental

### Apparatus and Software

All the experiments were performed at room temperature (25°C). The absorption data were recorded using the Agilent 8453 UV-Vis spectrophotometer equipped with a diode-array detector. A light box similar to the one used in a study by Damirchi et al. (30) was employed for digital-image-based colorimetric analysis. The dimensions of the light box were 18 × 25 × 17.5 cm (width × length × height) with a 3 × 3 cm window on

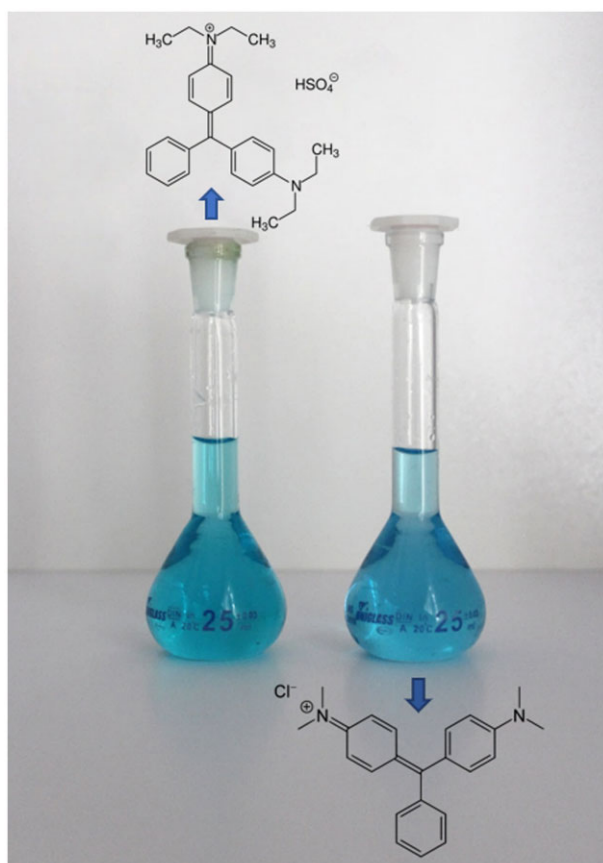


Figure 1. BG 6 mg/L (left solution) and MG 6 mg/L (right solution).

the front side. Six white LEDs mounted on the left and the right interior sides of the box were used as the light source. A quartz cuvette and a glass cuvette with 1 cm width were used as sample holders. To measure and adjust the pH, a digital pH meter (SL-901 Sana Electronics, Iran) was used. Images were captured by a Canon EOS 1300D digital camera.

MATLAB 8.6 (The MathWorks, Natick, USA) software was used for image processing and quantitative analysis of the data. RGB color values of the digital images were acquired by ImageJ software. Minitab 17 software was used for design of experiments and statistical tests.

### Reagents and Samples

Analytical grade of all chemicals was used in the experiments with no further purification. BG, MG, and Triton X-100 were supplied by Sigma-Aldrich (St. Louis, USA). Sodium acetate, acetic acid, and potassium chloride were purchased from Dr. Mojallali Co. (Tehran, Iran).

All the solutions were prepared using deionized water. A buffer solution of 0.1 mol/L of acetic-acetate was prepared by dissolving appropriate amounts of sodium acetate and acetic acid in 1.0 L water. Then, the pH was adjusted in 4. Stock solutions of BG and MG (50 mg/L) were prepared by dissolving 0.01 g of each dye in 50 mL of the prepared buffer solution and diluting them to 200 mL with the same buffer in volumetric flasks. Due to the photosensitivity and thermosensitivity of the dyes, the volumetric flasks were subsequently covered by aluminum foil to avoid light exposure and stored at 4°C. A 330 mmol/L of TX-100 solution was prepared by dissolving 2 mL of TX-100 in 10 mL water. In all the experiments, 50 µL of this solution was added to 2 mL of the solutions containing dye to form a micellar medium. The concentration of TX-100 in these solutions was 8.25 mmol/L, which is above the critical micelle concentration of this surfactant (0.22 mmol/L) (30).

### Method

To compare the behaviors of the dyes in the presence and absence of TX-100 micelle, MG and BG were individually analyzed in aquatic and micellar media. In the next step, quantitative colorimetric and spectrophotometric measurement of the dyes was performed. Calibration sets and prediction sets composed of binary mixtures of the dyes were designed according to the linear dynamic range of each dye for each method. The calibration sets were obtained by a five-level two-factor design from Minitab software. This design gave 25 runs for the calibration sets. Since orthogonality is not necessary for designing the prediction sets, these sets were obtained by a random design containing nine runs that were different from the calibration runs. The concentration ranges at which the sets were designed were spanned in the linear dynamic range of the dyes obtained by the univariate analysis.

Solutions of the binary mixtures of MG and BG were prepared by adding appropriate volumes of their stock solutions in 25 mL volumetric flasks and diluting them with acetic-acetate buffer (0.1 mol/L). For digital-image-based colorimetric analysis, 2 mL of the intended solution was transferred to a glass cuvette, and then it was placed inside the light box. Images of aqueous solutions were taken by the camera before adding micelle. Due to the gradual change in the color of BG in the presence of TX-100 micelle, the images of micellar solutions were taken 20 min after adding micelle, at which the aforementioned trend had been ended (30). After capturing, the original images were

transferred to MATLAB and ImageJ software to obtain the RGB color histogram and pixel values. Quantitative measurements using PLS regression were performed in MVC1 toolbox in MATLAB (31).

For spectrophotometric analysis, the solution preparation procedure was the same as colorimetric analysis. The absorption spectra of the dye solutions in the quartz cuvette were recorded before adding micelle and again 20 min after that. The obtained absorbance data were processed using MVC1 toolbox in MATLAB.

### Image Processing

Original images that were recorded by the camera were cropped to specific dimensions. After that, the images were inserted to MATLAB software using the *imread* function. These images were split into three layers of matrixes using the *image* function. Each of the matrixes belonged to one of the RGB channels. Then, the histogram values for each channel were obtained using the *imhist* function.

To extract the mean pixel values for the RGB channels, the cropped images were inserted into ImageJ software and the *Histogram* option was selected from the *Analyze* tab.

### Statistical Evaluation

The methods were evaluated by calculating statistical parameters including root-mean-square errors for prediction set (RMSEP), root-mean-square errors for calibration set (RMSEC) coefficient of determination ( $R^2$ ), and relative errors of prediction (REP) (32).

The number of the latent variables for the PLS regression was selected based on a leave-one-out cross-validation method. This number provided the minimum root-mean-square errors of cross-validation (RMSECV) (32).

LOD and LOQ for univariate analysis were calculated as follows:

$$LOD = \frac{3\sigma}{m} \quad (1)$$

$$LOQ = \frac{10\sigma}{m} \quad (2)$$

where  $\sigma$  is the standard deviation of blank, and  $m$  is the slope of the calibration curve.

To assess the prediction ability of the model, the ratio performance to deviation (RPD) was calculated as follows:

$$RPD = \frac{SD}{RMSEP} \quad (3)$$

where  $SD$  is the standard deviation of the reference data, and  $RMSEP$  is the root-mean-square errors of the prediction set. It has been suggested that a model is good for screening with a  $RPD > 3$ , good for quality control with a  $RPD > 5$ , and excellent for all analytical tasks with a  $RPD > 8$  (33).

### Real Samples Analysis

Fish-pond water and textile wastewater samples were collected from a fish farm and a textile factory near the city of Mashhad in Iran, respectively. First, 25 mL of each sample was filtered with Whatman grade 40 filter-paper to eliminate any suspended matter. Then, each of the samples was added to 10 mL

potassium chloride solution (2 M) and diluted to 200 mL with acetic-acetate buffer (0.1 M). Eventually, samples were spiked with standards of MG and BG and submitted to the measurement procedure already described.

## Results and Discussion

### MG and BG Analysis in Aquatic and Micellar Media

Many of the characteristics of MG and BG—for example, their chemical structures and absorption spectra—are strongly similar to one another. Also, the high similarity between the colors of these two dyes can be observed in their RGB color histogram. Figure 2 displays the RGB color histograms of MG and BG in aquatic and micellar media. Region of interest (ROI) for the images was defined as a fixed  $70 \times 70$  pixels area of the sample image. As can be seen, the RGB curves in the histogram of MG and BG (especially the red channels and the green channels) exhibit a high degree of overlap in aquatic environments. This amount of overlap will hinder the calibration methods (for example, PLS) from having a proper function. When micelle is added to the dye solutions, a small shift to the right side of the histogram has occurred on the red and the green curves of MG, whereas the blue curve has moved to the left side. It can be seen that by adding micelle, the red and the green curves of BG have shifted to the left side and the blue curve has shifted to the right side. These shifts are the result of slight changes in the colors of the dyes' solutions after micelle addition. The partial separation in the RGB curves of the two dyes caused by adding micelle can improve the measurements. The original reason for such phenomena can be elucidated by studying the absorption spectra of the dyes.

Figure 3 demonstrates the MG and BG individual and mixture absorption spectra in aqueous and micellar solutions from the wavelength 350 to 700 nm. As in the histograms, it can be seen that the spectra of the dyes in aqueous solutions are highly overlapped in this region but partially deconvoluted in micellar media. After adding TX-100 micelle to the solutions, a bathochromic shift has occurred at the absorption maximum of BG from 625 to 634 nm, accompanied by an increase in the

absorbance value at the  $\lambda_{max}$ . A similar bathochromic shift from 618 to 624 nm is observed at the absorption maximum of MG, and the absorbance value at its  $\lambda_{max}$  has been reduced.

The bathochromic shift can be caused by a change in the microenvironment available to MG and BG after adding micelle, leading to a decrease in the energy gap between the HOMO and LUMO orbitals of these dyes (34). Since MG and BG are considered to be cationic dyes, and TX-100 is a nonionic surfactant, different types of interactions between each dye and TX-100 are likely to happen. It appears that the BG molecules get incorporated within TX-100 micellar aggregates, resulting to an increase in the solubility and stability of this dye and, eventually, a rise in the absorbance value at its  $\lambda_{max}$ . On the other hand, MG molecules present a lower tendency for solubilization in the micellar aggregates, and the absorbance value at the  $\lambda_{max}$  decreases due to the formation of moderately soluble precipitate of MG. Similar observations can be found in studies on the dye-surfactant interactions (35–38).

### Analytical Parameters

The univariate analysis of the dyes is important for preparing the standard solutions for the calibration and prediction sets because that the concentration of each compound must be bound to their respective linear dynamic range (39). The calibration curves of the univariate analysis of MG and BG in aquatic and micellar media were plotted to determine the linear ranges, limits of detection (LODs), and limits of quantification (LOQs). For this purpose, standard solutions of MG and BG were analyzed by the camera and the spectrophotometer. For spectrophotometric analysis, the plots were conveniently obtained using the absorbance values at the  $\lambda_{max}$  of each dye. To enhance the repeatability and sustainability of the colorimetric analysis, a specific manual setting was adjusted to the camera in all the experiments. The optimum conditions for image acquisition are summarized in Table 1. The calibration curves of the univariate analysis for colorimetric method were plotted using the mean pixel value of each channel (red, blue, and green) modified by subtraction from the mean pixel value of the blank.

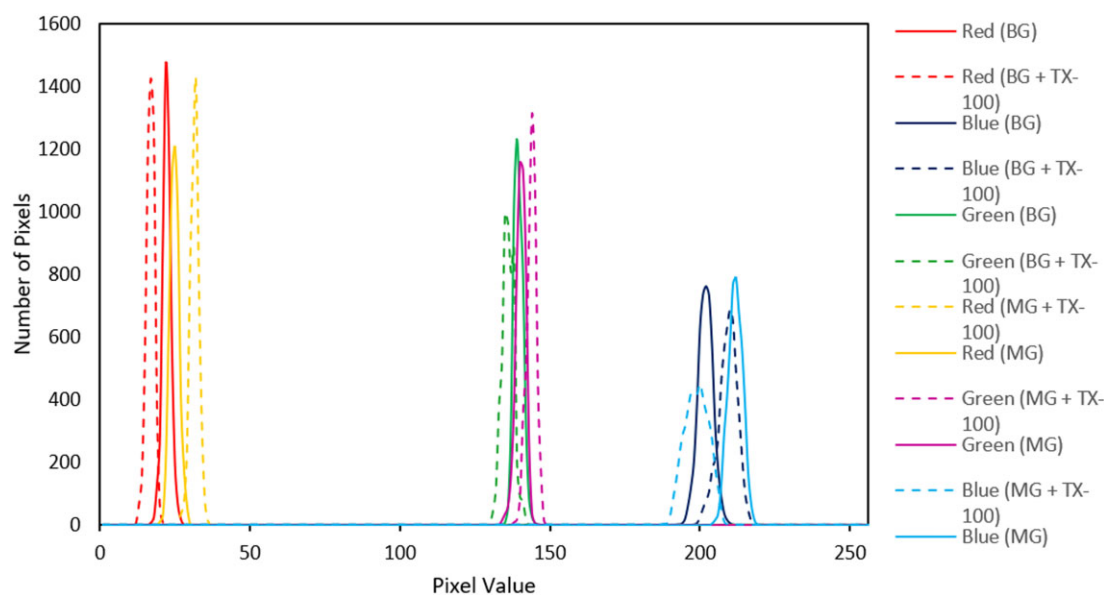


Figure 2. RGB color histogram of (a) MG (6 mg/L) and (b) BG (6 mg/L) in aquatic and micellar media. TX-100 concentration in solutions: 8.25 mmol/L.



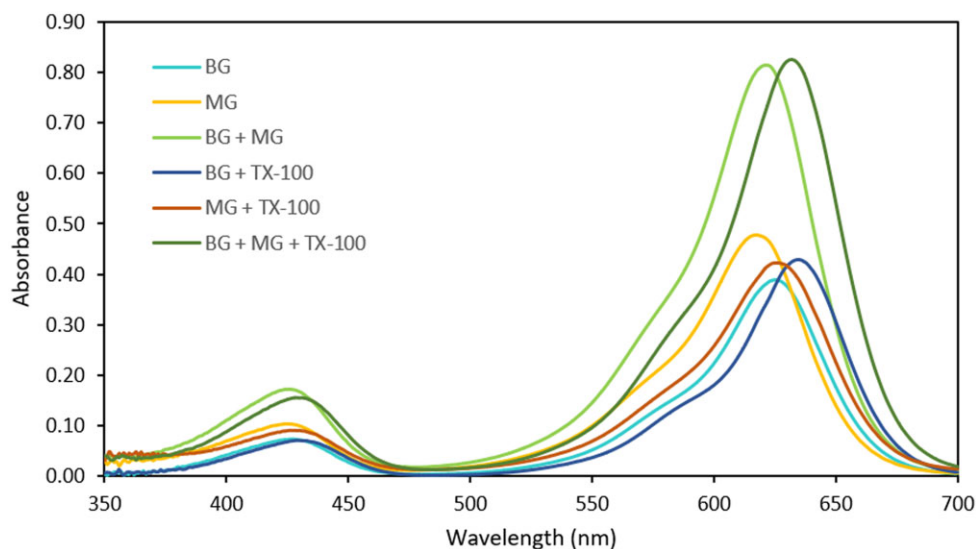


Figure 3. UV-Vis absorption spectra of MG (6 mg/L) and BG (3 mg/L) in aqueous and micellar solutions. TX-100 concentration in solutions: 8.25 mmol/L.

Table 1. Optimum conditions for image acquisition

Option	Aperture	Shutter speed	ISO	White balance	Distance <sup>a</sup>
Optimum condition	f/4	1/500	100	Fluorescence	15 cm

<sup>a</sup>Distance between the sample and the camera.

Relative standard deviations of standard samples were calculated using six replicants. Analytical figures of merits for both methods are summarized in Table 2. According to Table 2, the spectrophotometric analysis gave wider linear ranges and lower LODs and LOQs.

#### ROI Optimization

Figure 4 shows the RGB histograms of a sample originated from different regions of interest (ROIs). As can be seen, small ROI (10 × 10 pixels area) leads to very narrow RGB curves with noise. Likewise, the RGB curves of the large ROI (170 × 170 pixels area) are noisy, but they are also wider.

As the ROI dwindles, the total number of the pixels decreases. Therefore, the RGB curves in the histogram become narrower. The narrow RGB curves are not suitable for multivariate calibrations as they provide few data points. In large ROIs, the total number of the pixels and, subsequently, their distributions grow larger. This gives RGB curves with a high amount of noise, which can cause errors in the measurements. Here, a 70 × 70 pixels area gave sharp curves without noise; thus, it was considered the optimum ROI for multivariate calibrations.

#### Formation of the Calibration and Prediction Matrixes

To use multivariate calibration methods, e.g., PLS for quantitative analysis, a calibration set and a prediction set are needed. Each set consists of several mixtures with specific concentrations of the analytes. The compositions of the calibration and prediction sets for experimental analysis are presented in Table 3. To set the most accurate measurement conditions, the following points were taken into account for preparing the calibration and prediction sets: (1) Since the linear ranges for the

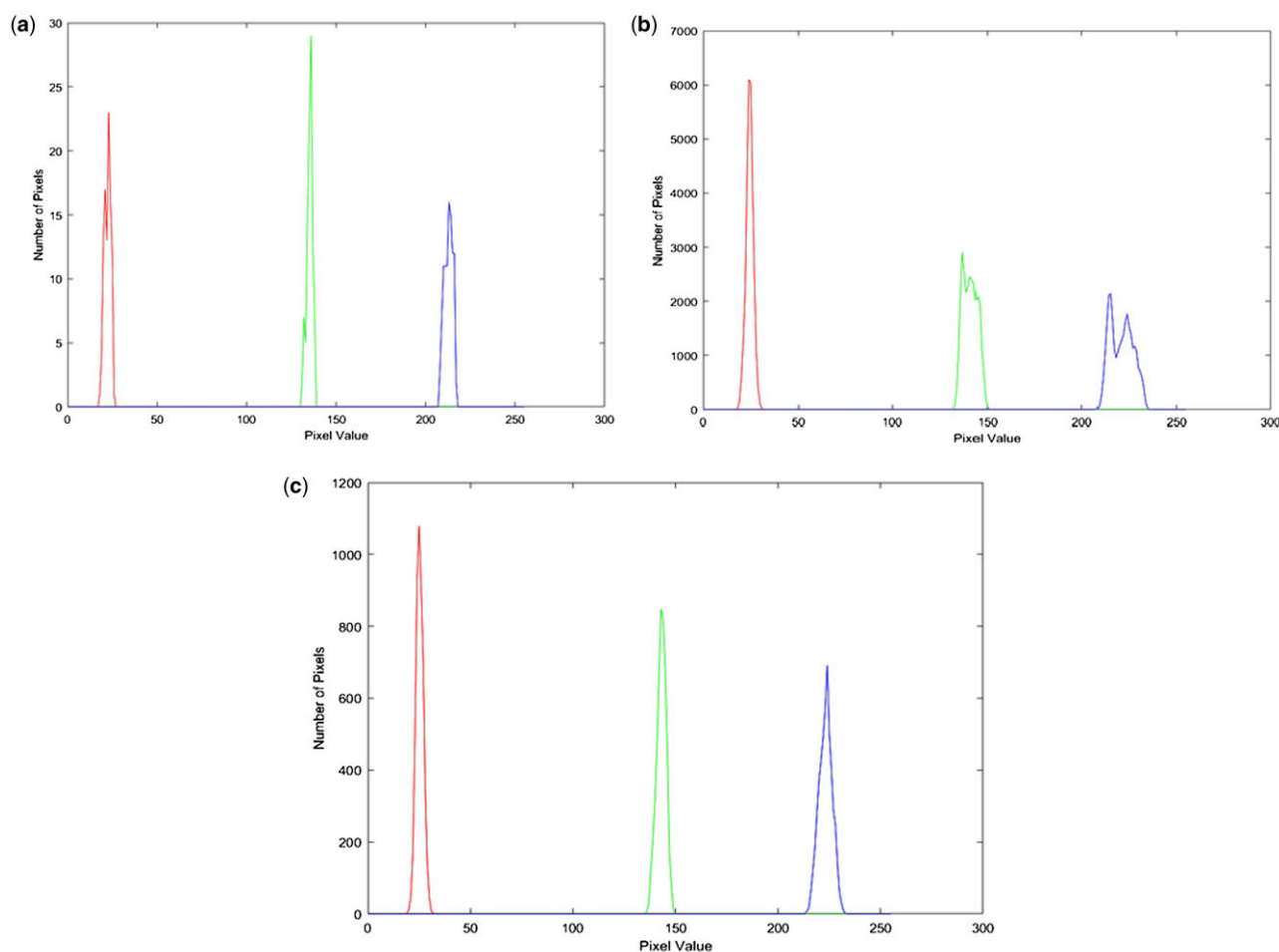
channels of RGB were different, the concentration range in which all of the channels were linear was considered for the calibration and prediction sets of the colorimetric analysis. (2) The prediction sets were designed with random concentrations that were not used in the calibration sets. (3) Initially, there were 25 samples in the calibration set of the spectrophotometric analysis. After performing a statistical *F*-test for regression analysis, the sample numbers 7, 9, 13, 17, 19, and 25 were identified as outliers by the *F*-ratios above 1 (Figure 5). Therefore, they were omitted from the calibration set, and the 19 remaining samples were used for further measurements. To create identical conditions for both spectrophotometric and colorimetric analysis, the sample numbers 1, 2, 6, 7, 24, and 25 of the calibration set for the colorimetric analysis that had the lowest and highest responses were removed to achieve a 19-sample set. The *F*-ratios of the statistical *F*-test showed no outlier for these samples.

The histogram values and absorbance values obtained from the calibration and prediction experiments were collocated as follows to form specific matrixes to be used in the PLS model.

The sets generated a 351 × 19 matrix for the calibration and a 351 × 9 matrix for the prediction in spectrophotometric analysis, according to the examined wavelength range (350 to 700 nm), which included 351 data points. The matrix production for colorimetric analysis was different. There were three vectors with the length of 256 in the histogram of every sample, each belonging to one of the channels of RGB. These vectors were aligned together to form a single vector with a length of 768, which was used as an input for every sample. Then, matrixes with the size of 768 × 19 and 768 × 9 were attained for the calibration and prediction, respectively.

**Table 2.** Analytical figures of merit for the univariate analysis

Dye	Medium	Method	Equation ( $R^2$ )	Linear range <sup>a</sup>	LOD <sup>a</sup>	LOQ <sup>a</sup>	RSD, %	
MG	Aquatic	Spectrophotometry	$0.076x + 0.004$ (0.99)	0.10–12.00	0.06	0.19	0.25	
		Colorimetry	R channel	$6.73x + 12.14$ (0.99)	0.50–10.00	0.08	0.26	1.15
			G channel	$1.22x + 9.89$ (0.98)	0.50–10.00	0.09	0.29	1.22
			B channel	$1.73x + 6.84$ (0.97)	0.50–6.00	0.10	0.33	1.33
	Micellar	Spectrophotometry	$0.068x + 0.008$ (0.99)	0.10–10.00	0.06	0.19	0.27	
		Colorimetry	R channel	$6.52x + 9.28$ (0.99)	0.50–10.00	0.08	0.26	0.98
G channel			$2.32x + 4.52$ (0.98)	0.50–6.00	0.10	0.33	1.02	
BG	Aquatic	Spectrophotometry	R channel	$0.11x + 0.05$ (0.99)	0.10–12.00	0.02	0.06	0.28
			G channel	$7.67x + 16.77$ (0.98)	0.50–8.00	0.10	0.33	1.17
		Colorimetry	G channel	$1.69x + 7.89$ (0.97)	0.50–8.00	0.10	0.33	1.76
			B channel	$1.93x + 9.91$ (0.97)	0.50–8.00	0.10	0.33	1.83
	Micellar	Spectrophotometry	R channel	$0.14x + 0.01$ (0.99)	0.10–15.00	0.01	0.03	0.19
			G channel	$6.87x + 21.61$ (0.99)	0.50–10.00	0.09	0.29	1.25
		Colorimetry	G channel	$3.43x + 1.57$ (0.99)	0.50–6.00	0.08	0.26	1.40
			B channel	$4.9x + 5.53$ (0.99)	0.50–6.00	0.08	0.26	1.41

<sup>a</sup> mg/L.**Figure 4.** Histograms of a sample (mixture of MG: 3 mg/L and BG: 2 mg/L) with different ROIs. (a)  $10 \times 10$  pixels area, (b)  $170 \times 170$  pixels area, and (c)  $70 \times 70$  pixels area.

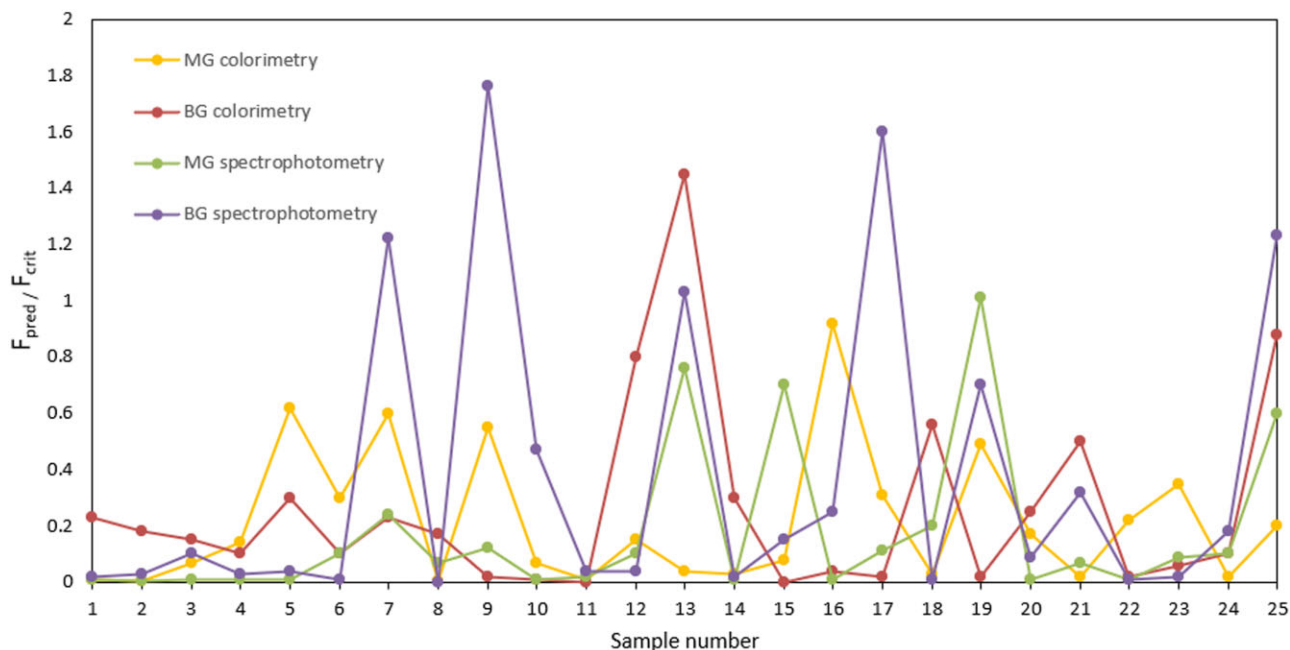
#### Quantitative Measurement of MG and BG

The results of the experimental analysis are given in Table 4, and the plots of predicted values versus real values for both

methods are displayed in Figure 6. It can be seen that micelle addition has made a remarkable improvement in the analysis of the dyes. As expected, the proposed colorimetric method

**Table 3.** Composition of calibration and prediction sets for experimental analysis (concentrations of MG and BG: mg/L)

Mixture number	Calibration for spectrophotometry		Prediction for spectrophotometry		Calibration for colorimetry		Prediction for colorimetry	
	MG	BG	MG	BG	MG	BG	MG	BG
1	2.00	1.00	2.50	3.30	0.50	0.50	1.88	1.68
2	4.00	1.00	5.00	3.20	1.00	0.50	2.15	2.55
3	6.00	1.00	6.90	1.20	2.00	0.50	0.86	1.92
4	8.00	1.00	8.90	4.00	3.00	0.50	2.55	3.10
5	10.00	1.00	9.50	2.40	4.0	0.50	2.65	1.66
6	2.00	2.00	5.40	4.70	0.50	1.50	1.23	2.14
7	4.00	2.00	2.40	1.70	1.00	1.50	1.62	2.64
8	6.00	2.00	9.20	2.90	2.00	1.50	2.75	2.95
9	8.00	2.00	2.50	1.10	3.00	1.50	3.22	2.75
10	10.00	2.00			4.00	1.50		
11	2.00	3.00			0.50	2.50		
12	4.00	3.00			1.00	2.50		
13	6.00	3.00			2.00	2.50		
14	8.00	3.00			3.00	2.50		
15	10.00	3.00			4.00	2.50		
16	2.00	4.00			0.50	3.50		
17	4.00	4.00			1.00	3.50		
18	6.00	4.00			2.00	3.50		
19	8.00	4.00			3.00	3.50		
20	10.00	4.00			4.00	3.50		
21	2.00	5.00			0.50	5.00		
22	4.00	5.00			1.00	5.00		
23	6.00	5.00			2.00	5.00		
24	8.00	5.00			3.00	5.00		
25	10.00	5.00			4.00	5.00		

**Figure 5.** Statistical  $F$ -test results for calibration sets of the colorimetric and spectrophotometric analysis.

combined with the PLS regression failed to accurately determine the amounts of MG and BG simultaneously in aquatic media due to the high overlap in the RGB curves in the color histogram of the dyes. This can be concluded from the low values of  $R^2$  and high percentages of REP for the analysis of the

dyes in aquatic media. When micelle is added, the RGB curves of the dyes are separated, and the method's function has been improved. The same trend can be observed in the spectrophotometric analysis of the dyes. The spectral deconvolution related to micelle addition has enhanced the method's performance.

Table 4. Results of experimental analysis

Method	Matrix	Dye	LVs	RMSEC	RMSECV	R <sup>2</sup>	RMSEP	REP, %	RPD
Colorimetry	Aquatic media	MG	3	0.26	0.19	0.64	0.43	20.56	1.67
		BG	3	0.55	0.42	0.39	0.82	36.73	0.62
	Micellar media	MG	3	0.11	0.10	0.95	0.14	6.56	5.14
		BG	3	0.12	0.16	0.93	0.14	6.38	3.64
Spectrophotometry	Aquatic media	MG	3	0.28	0.13	0.96	0.52	8.99	5.36
		BG	2	0.89	0.33	0.53	1.24	43.01	0.93
	Micellar media	MG	3	0.19	0.11	0.99	0.27	4.61	10.22
		BG	2	0.14	0.19	0.98	0.14	5.24	8.28

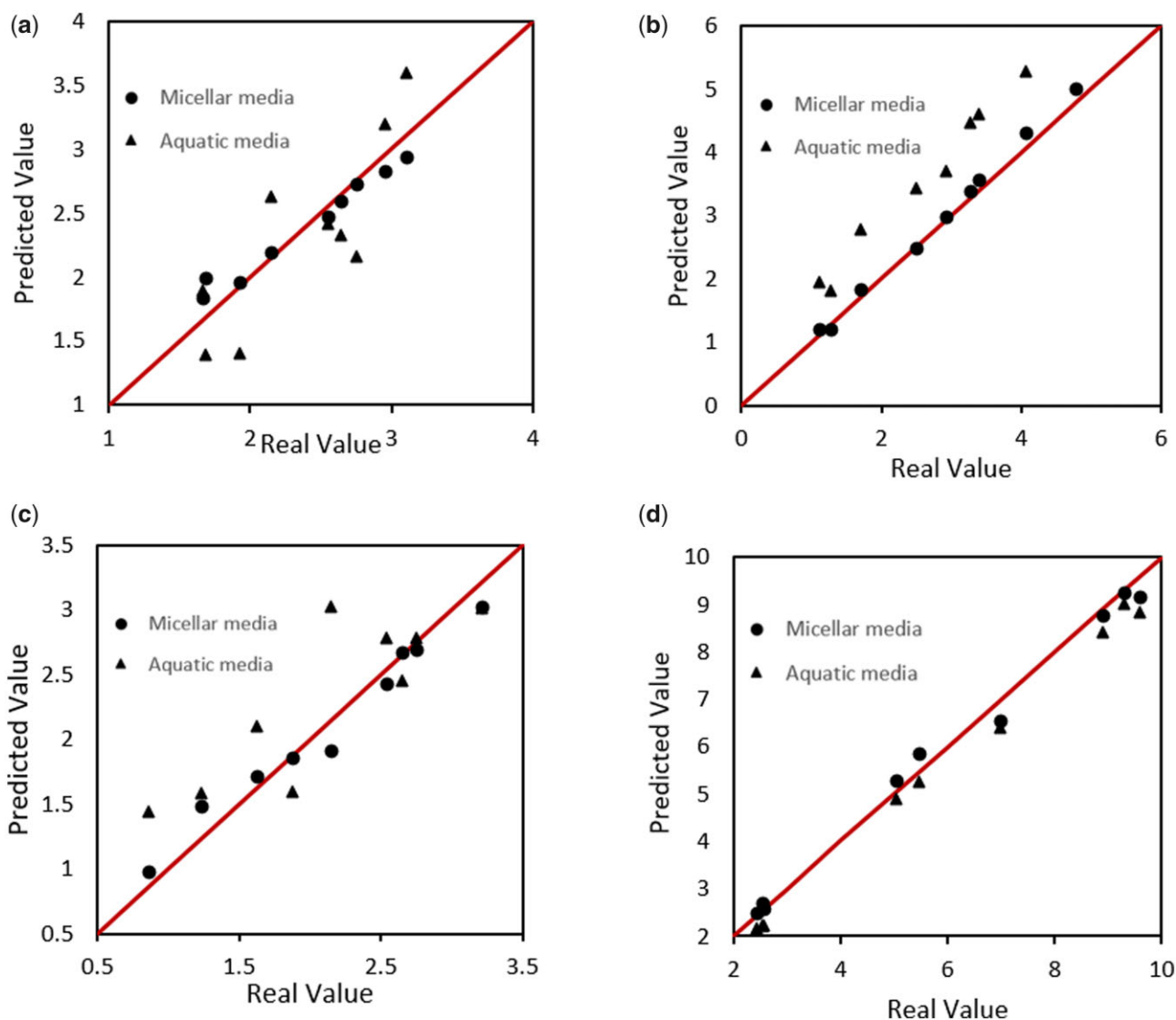


Figure 6. Scatter plots of predicted values versus real values for BG in (a) colorimetric and (b) spectrophotometric analysis; and for MG in (c) colorimetric and (d) spectrophotometric analysis (real values and predicted values: mg/L).

Additionally, the good agreement between the results of the colorimetric analysis and the spectrophotometric analysis as a reference method indicates that the proposed method is reliable.

The RPD values calculated for the colorimetric analysis of the dyes in aquatic media are considerably low. This can be interpreted as this method not having an efficient performance

in such media. By adding micelle, the RPD values significantly increased, falling within the acceptable range. The RPD value for the colorimetric analysis of BG is above 3, which shows that this method is good for screening, and the RPD value for the colorimetric analysis of MG is above 5, showing that this method is good for quality control of this dye. The RPD values for the spectrophotometric analysis of the dyes in micellar media are both



above 8, which indicates that this method is good for all analytical tasks for these dyes.

Figure 7 shows the elliptical joint confidence region (EJCR) plots for both methods performed in micellar media. These plots, which were acquired from MVC1 toolbox in MATLAB, are applied to evaluate the security and the precision of the methods. They demonstrate the estimated intercept versus the slope, and if the points [0,1] lie inside the graph, then bias is absent. As can be observed, all the plots included the ideal [0,1] points. This means that the results are not biased, and the methods are secure for the respective purposes.

### Real Samples Analysis

Simultaneous determination of MG and BG has been carried out in two different types of real sample, including fish-pond water and textile wastewater, to evaluate the method's reliability in the presence of unknown amounts of interferences. The results of relative recovery study for both intra-day and inter-day (5 days) analysis of the dyes implemented in the micellar media, respectively, are shown in Tables 5 and 6. The closeness of relative recoveries to 100% is satisfactory, which proves that the matrix effect in determination of the analytes is insignificant. To assess this factor, a statistical t-test with a 99% confidence level has been done using Minitab software. The results

presented in Table 7 show that the P-values calculated from intra-day relative recoveries were all above the significance level or  $\alpha$  (0.01). This provides evidence that the relative recoveries were not different from the hypothesized mean, which was considered to be 100. On the other hand, the P-values of inter-day analysis were significantly lower than  $\alpha$ , showing that the relative recoveries had a considerable difference from 100. This can be related to the thermosensitive nature of the dyes. After keeping the samples with added dyes for 5 days, the fluctuations in temperature affected the measurements. It can be concluded that the measurements must be done immediately after the dyes are added.

### Conclusions

In this study, MG and BG were simultaneously determined using a colorimetric method coupled with a multivariate calibration model. This method has employed the RGB color histogram of the dyes for the analysis. As was observed, the RGB curves in the histograms were highly overlapped because both dyes exhibit similar a bluish-green tint. Adding Triton X-100 micelle to the solutions was an effective approach as it could partially separate the RGB curves and improve the method's performance. The method yielded adequately accurate results for the analysis

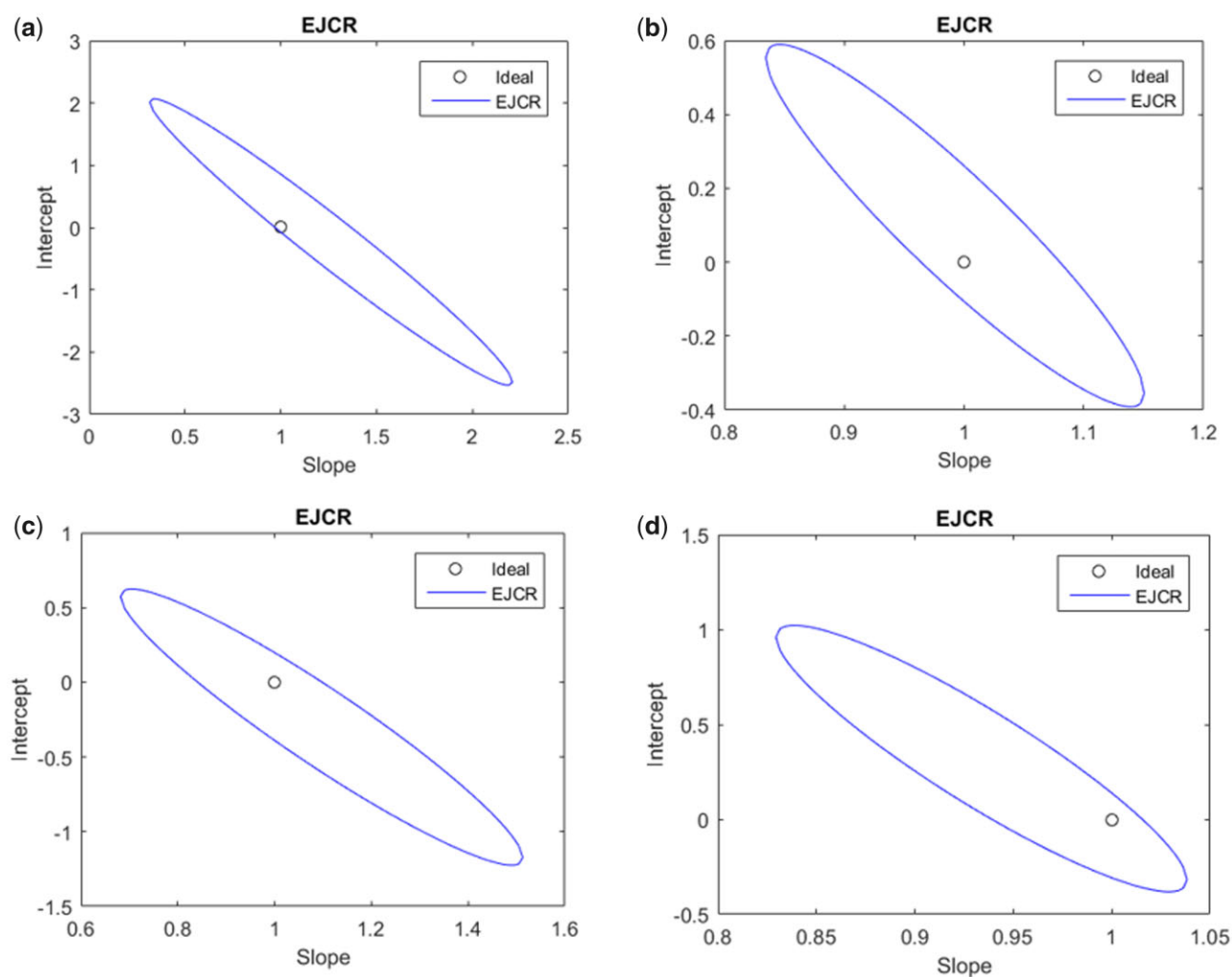


Figure 7. EJCR plots for the colorimetric analysis of (a) BG and (c) MG, and spectrophotometric analysis of (b) BG and (d) MG.

**Table 5.** Relative recovery study of real samples (intra-day)

Method	Sample matrix	Sample number	Malachite green				Brilliant green			
			Added <sup>a</sup>	Found <sup>a</sup>	Recovery, %	RSD, %	Added <sup>a</sup>	Found <sup>a</sup>	Recovery, %	RSD, %
Colorimetry	Textile wastewater	1	0	1.28	ND <sup>b</sup>	1.25	0	1.18	ND	1.66
		2	1	2.25	97	1.18	1	2.25	107	2.05
		3	2	3.14	93	2.09	2	3.20	101	1.79
		4	3	4.10	94	1.41	3	4.06	96	1.96
	Fish-pond water	5	0	–	ND	–	0	–	ND	–
		6	1	0.92	92	1.12	1	1.02	102	1.45
		7	2	1.82	91	1.22	2	2.14	107	1.57
		8	3	2.79	93	0.97	3	3.15	105	1.94
Spectrophotometry	Textile wastewater	1	0	1.40	ND	0.77	0	1.05	ND	0.79
		2	1	2.41	101	0.52	1	1.99	94	0.46
		3	2	3.44	102	0.33	2	3.03	99	0.68
		4	3	4.28	96	0.63	3	4.20	105	0.84
	Fish-pond water	5	0	–	ND	–	0	–	ND	–
		6	1	0.95	95	0.76	1	0.96	96	0.92
		7	2	1.94	97	0.39	2	2	100	0.97
		8	3	2.94	98	0.41	3	3.09	103	0.88

<sup>a</sup>Concentration unit: mg/L.<sup>b</sup>ND = Not detected.**Table 6.** Relative recovery study of real samples (inter-day)

Method	Sample matrix	Sample number	Malachite green				Brilliant green			
			Added <sup>a</sup>	Found <sup>a</sup>	Recovery, %	RSD, %	Added <sup>a</sup>	Found <sup>a</sup>	Recovery, %	RSD, %
Colorimetry	Textile wastewater	1	0	1.25	ND <sup>b</sup>	1.85	0	0.92	ND	1.90
		2	1	2.19	94	1.64	1	1.87	95	2.12
		3	2	3.17	96	2.06	2	2.90	96	1.86
		4	3	4.02	92	1.98	3	3.77	95	1.59
	Fish-pond water	5	0	–	ND	–	0	–	ND	–
		6	1	0.93	93	1.19	1	0.91	91	1.99
		7	2	1.82	91	1.44	2	1.89	94	1.75
		8	3	2.83	94	1.12	3	2.80	93	1.65
Spectrophotometry	Textile wastewater	1	0	1.32	ND	0.77	0	0.98	ND	1.01
		2	1	2.25	93	0.87	1	1.88	90	0.95
		3	2	3.16	92	0.94	2	2.93	97	1.12
		4	3	4.09	92	0.81	3	4.05	102	0.74
	Fish-pond water	5	0	–	ND	–	0	–	ND	–
		6	1	0.95	95	0.78	1	0.93	93	0.86
		7	2	1.92	96	0.69	2	1.86	94	0.89
		8	3	2.86	95	0.81	3	2.85	95	0.75

<sup>a</sup>Concentration unit: mg/L.<sup>b</sup>ND = Not detected.**Table 7.** Results of the statistical t-test for relative recovery percentages

Method	Analyte	Intra-day		Inter-day	
		t-value	P-value	t-value	P-value
Spectrophotometry	MG	–1.61	0.168	–8.77	0.001
	BG	–0.30	0.779	–3.91	0.003
Colorimetry	MG	–1.91	0.015	–9.33	0.001
	BG	1.73	0.144	–8.21	0.001

of the dyes in micellar media. The effect of micelle addition studied by a spectrophotometric method also indicated reduced overlapped spectra and improved results. It proved that this technique is advantageous for simultaneous analysis of dyes

even with very similar colors. As opposed to many complex separation methods, e.g., HPLC, this method is very simple and does not need any tedious sample preparation steps. The method takes advantage of the PLS model, a very powerful multivariate calibration method, for a rapid and nondestructive measurement. Furthermore, this method employs an inexpensive instrument, i.e., a digital camera, for quantitative analysis. The relative recovery study of the real samples also confirmed insignificant interferences with other unknown compounds in the matrix.

### CRedit Author Statement

Negar Qashqai: Investigation, Formal analysis, Writing—original draft, Writing—review and editing. Tahereh Heidari:

Conceptualization, Formal analysis, Methodology, Writing—review and editing.

## Acknowledgments

The authors gratefully appreciate Ferdowsi University of Mashhad, Mashhad, Iran, for the financial support of this research.

## Conflict of Interest

All authors declare no conflict of interest.

## Funding

The financial aid for this research project was provided by Ferdowsi University of Mashhad.

## References

- Behbahani, M. (2020) *J. AOAC Int.* **103**, 227–234. doi:10.5740/jaoacint.19-0119
- Sobhi, H.R., Ghambarian, M., Behbahani, M., & Esrafil, A. (2017) *J. Chromatogr. A* **1518**, 25–33. doi:10.1016/j.chroma.2017.08.064
- Behbahani, M., Bagheri, S., Omidi, F., & Amini, M.M. (2018) *Microchim. Acta* **185**, 1–8. doi:10.1007/s00604-018-3038-5
- Behbahani, M., Omidi, F., Kakavandi, M.G., & Hesam, G. (2017) *Appl. Organomet. Chem.* **31**, e3758. doi:10.1002/aoc.3758
- Behbahani, M., Veisi, A., Omidi, F., Noghrehabadi, A., Esrafil, A., & Ebrahimi, M.H. (2018) *Appl. Organometal. Chem.* **32**, e4134. doi:10.1002/aoc.4134
- Aladaghlo, Z., Fakhari, A., & Behbahani, M. (2016) *J. Chromatogr. A* **1462**, 27–34. doi:10.1016/j.chroma.2016.07.084
- Che Sulaiman, I.S., Chieng, B.W., Osman, M.J., Ong, K.K., Rashid, J.I.A., Wan Yunus, W.M.Z., Noor, S.A.M., Kasim, N.A.M., Halim, N.A., & Mohamad, A. (2020) *Microchim. Acta* **187**, 1–22. doi:10.1007/s00604-019-3893-8
- Liu, T., Zhang, S., Liu, W., Zhao, S., Lu, Z., Wang, Y., Wang, G., Zou, P., Wang, X., Zhao, Q., & Rao, H. (2020) *Sens. Actuat. B* **305**, 127524. doi:10.1016/j.snb.2019.127524
- Shi, C., Qian, J., Han, S., Fan, B., Yang, X., & Wu, X. (2018) *Food Chem.* **243**, 134–140. doi:10.1016/j.foodchem.2017.09.047
- de Oliveira Morais, P.A., de Souza, D.M., Madari, B.E., da Silva Soares, A., & de Oliveira, A.E. (2019) *Microchem. J.* **147**, 775–781. doi:10.1016/j.microc.2019.03.070
- de Sousa Fernandes, D.D., Romeo, F., Krepper, G., Di Nezio, M.S., Pistonesi, M.F., Centurión, M.E., de Araújo, M.C.U., & Diniz, P.H.G.D. (2019) *LWT* **100**, 20–27. doi:10.1016/j.lwt.2018.10.034
- de Sousa Fernandes, D.D., Romeo, F., Krepper, G., Di Nezio, M.S., Pistonesi, M.F., Centurión, M.E., de Araújo, M.C.U., & Diniz, P.H.G.D. (2016) *Anal. Methods* **8**, 7632–7637. doi:10.1039/C6AY02126C
- Vidal, M., Garcia-Arrona, R., Bordagaray, A., Ostra, M., & Albizu, G. (2018) *Talanta* **184**, 58–64. doi:10.1016/j.talanta.2018.02.111
- Ostad, M.A., Hajinia, A., & Heidari, T. (2017) *Microchem. J.* **133**, 545–550. doi:10.1016/j.microc.2017.04.031
- Gonçalves Dias Diniz, P.H. (2020) *J. Chemom.* **34**, e3242. doi:10.1002/cem.3242
- Shariati-Rad, M., Irandoust, M., & Mohammadi, S. (2016) *Chemom. Intell. Lab. Syst.* **158**, 48–53. doi:10.1016/j.chemolab.2016.08.015
- Bhattacharyya, K.G., & Sarma, A. (2003) *Dyes. Pigm.* **57**, 211–222. doi:10.1016/S0143-7208(03)00009-3
- Baek, M.H., Ijagbemi, C.O., Se-Jin, O., & Kim, D.S. (2010) *J. Hazard Mater.* **176**, 820–828. doi:10.1016/j.jhazmat.2009.11.110
- Es'haghi, Z., Khooni, M.A.-K., & Heidari, T. (2011) *Spectrochim. Acta. A Mol. Biomol. Spectrosc.* **79**, 603–607. doi:10.1016/j.saa.2011.03.042
- Lin, Z.Z., Zhang, H.Y., Peng, A.H., Lin, Y.D., Li, L., & Huang, Z.Y. (2016) *Food Chem.* **200**, 32–37. doi:10.1016/j.foodchem.2016.01.001
- Srivastava, S.J., Singh, N.D., Srivastava, A.K., & Sinha, R. (1995) *Aquat. Toxicol.* **31**, 241–247. doi:10.1016/0166-445X(94)00061-T
- Vigneshpriya, D., Krishnaveni, N., Renganathan, S., & Sri Sakthi Priyadarshini, R. (2020) *Int. J. Phytoremediat.* **22**, 819–826. doi:10.1080/15226514.2019.1710816
- Méndez, A., Fernández, F., & Gascó, G. (2007) *Desalination* **206**, 147–153. doi:10.1016/j.desal.2006.03.564
- Mane, V.S., Mall, I.D., & Srivastava, V.C. (2007) *Dyes. Pigm.* **73**, 269–278. doi:10.1016/j.dyepig.2005.12.006
- Mane, V.S., Mall, I.D., & Srivastava, V.C. (2007) *J. Environ. Manage.* **84**, 390–400. doi:10.1016/j.jenvman.2006.06.024
- Hurtaud-Pessel, D., Couëdor, P., & Verdon, E. (2011) *J. Chromatogr. A* **1218**, 1632–1645. doi:10.1016/j.chroma.2011.01.061
- López-Gutiérrez, N., Romero-González, R., Plaza-Bolaños, P., Martínez-Vidal, J.L., & Garrido-Frenich, A. (2013) *Food Anal. Methods* **6**, 406–414. doi:10.1007/s12161-012-9456-9
- Pradel, J.S., & Tong, W.G. (2017) *Anal. Methods* **9**, 6411–6419. doi:10.1039/C7AY01706E
- Martens, H., & Næs, T. (1989) *Multivariate Calibration*, Wiley, New York, pp 440
- Damirchi, S., Maliheh, A.K.K., Heidari, T., Es'haghi, Z., & Chamsaz, M. (2019) *Spectrochim. Acta. A Mol. Biomol. Spectrosc.* **206**, 232–239. doi:10.1016/j.saa.2018.08.011
- Chiappini, F.A., Goicoechea, H.C., & Olivieri, A.C. (2020) *Chemom. Intell. Lab. Syst.* **206**, 104162. doi:10.1016/j.chemolab.2020.104162
- Brereton, R.G. (2000) *Analyst* **125**, 2125–2154. doi:10.1039/B003805I
- Williams, P. (2014) *NIR News* **25**, 22–26. doi:10.1255/nirn.1419
- Ahmed, S.A., Singh, U., & Seth, D. (2019) *J. Photochem. Photobiol. A* **376**, 247–254. doi:10.1016/j.jphotochem.2019.03.023
- Wang, N., & Zhao, M. (2016) *J. Dispers. Sci. Technol.* **37**, 190–195. doi:10.1080/01932691.2015.1039019
- Alehyen, S., Bensejjay, F., El Achouri, M., Pérez, L., & Infante, M.R. (2010) *J. Surfact. Detergents* **13**, 225–231. doi:10.1007/s11743-009-1161-3
- Muntaha, S.T., & Khan, M.N. (2014) *J. Mol. Liq.* **197**, 191–196. doi:10.1016/j.molliq.2014.05.008
- Nazar, M.F., Shah, S.S., & Khosa, M.A. (2010) *J. Surfact. Detergents* **13**, 529–537. doi:10.1007/s11743-009-1177-8
- Zhang, C.-H., Yun, Y.-H., Zhang, Z.-M., & Liang, Y.-Z. (2016) *Int. J. Biol. Macromol.* **87**, 290–294. doi:10.1016/j.ijbiomac.2016.02.066